

A Study of the Surface Area and Structure of Activated Alumina by Direct Observation

J. H. BOWEN

From the University College, Swansea, Wales

AND

R. BOWREY AND A. S. MALIN

From the University of New South Wales, Sydney, Australia

Received January 8, 1966

A commercial sample of activated alumina has been examined with the electron microscope. The micrographs suggest the presence of three types of pores: a well-ordered array of cylindrical micropores approximately circular in cross section, 27Å in diameter, and arranged hexagonally; two types of random macropores, those within the particles of alumina that make up the granules, and those between such particles.

INTRODUCTION

During research into the operation of fixed-bed adsorbers, it became necessary to estimate the shape and the size distribution of pores in a commercial activated alumina. From the nitrogen isotherm shown in Fig. 1 it is possible to obtain some general and qualitative information about pore shapes (1) and several methods exist for the calculation of a pore-size distribution if a pore model is known (2, 3, 4), or even if one is not known (5). None of these methods, however, provide direct evidence of pore structure, so work was undertaken, using the electron microscope, in an attempt to obtain unambiguous information about pore sizes, voidages, and surface areas.

The activated alumina was an 8/16 B.S. grade of commercial origin, complete manufacturing details of which were not available. It was reported that the activated material was obtained from a precipitated multiple hydrate of alumina which was substantially X-ray amorphous but contained an easily recognizable proportion of

the monohydrate boehmite of small crystalline size. The precipitate was activated at a temperature of about 400°C. It seemed likely that the pore structure derived from the boehmite fraction would be regular but that the structure derived from the X-ray amorphous fraction would be either regular or irregular depending upon whether the absence of an X-ray pattern was the result of an exceptionally small crystalline size or that of a truly amorphous structure. It would also depend on the changes that took place during the first stages of activation when, possibly, considerable rehydration to boehmite could occur (6).

An analysis of the alumina showed Al₂O₃, 84.99% by wt; H₂O, 11.76%; SO₃, 3.25%.

The Structure of Alumina

A considerable amount of work has been carried out on the structure of alumina both in its hydrated state and during its dehydration. Electron micrographs and electron diffraction patterns previously ob-

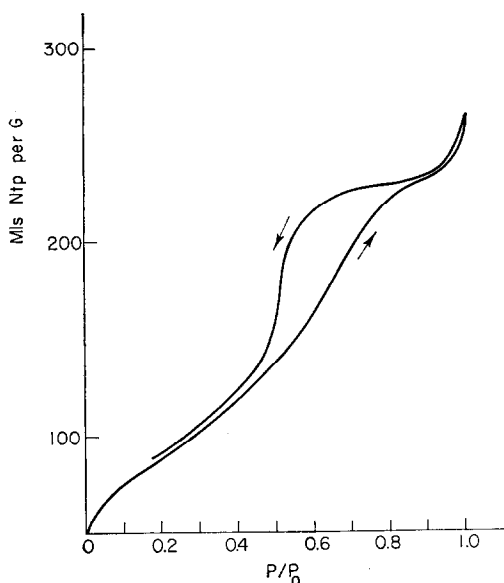


Fig. 1. Adsorption isotherm for nitrogen on the commercial alumina at the boiling point of liquid nitrogen at 1 atm [ref. (15)]. Abscissa, relative pressure of nitrogen; ordinate, volume of nitrogen referred to NTP adsorbed on 1 gram of solid.

tained (7, 8), showed a variety of structures depending on the precise conditions under which the hydrate was precipitated and subsequently treated. Structures made up of agglomerates of spherical particles, of fibrils, and of platelike layers are reported.

There is substantial agreement among several workers (6, 9, 10) about the behavior of the alumina trihydrates when heated. At about 150°C, decomposition to an anhydrous form starts. In the presence of this released moisture, above 150°C, rehydration to boehmite occurs. Boehmite persists until temperatures above 450°C are reached, when dehydration to a form of anhydrous alumina occurs once more.

de Boer (6) explains the pore structure in activated alumina derived from trihydrates as arising from the rupture of the lattice which occurs when the initial water of dehydration cannot diffuse away rapidly enough. At first, the pressure of released water builds up within the lattice and rehydration to boehmite occurs under this hydrothermal treatment. Eventually, the

lattice breaks along planes of weakness, which in the case of dehydrated gibbsite are (001) planes, and the first pores are formed. The structure at this stage is thought to consist of layers of alumina about 200 Å thick separated by parallel-sided fissures about 50 Å wide. The rupture occurs at a temperature of 180°C and heating beyond that point causes the planes to break into rods parallel to the first planes and to each other. The new fissures produced are thought to be about 10 Å in width and contribute the bulk of the surface area.

None of the above work suggested cylindrical pores, but their existence in thick oxide layers obtained by anodizing aluminum has been established (11). Some previous results (12) using a sample of the commercial alumina being investigated were not incompatible with the presence of cylindrical pores.

EXPERIMENTAL PROCEDURE

One manufacturer's batch of $\frac{8}{16}$ B.S. grade of activated alumina was used for all experiments. Adsorbates picked up during storage were eliminated by heating to 300°C for 1 hr at which temperature no changes in structure were expected in a material activated at 400°C.

Direct transmission electron microscopy was used for the examination since two-stage replica techniques (13) have poor replicating resolutions (>100 Å) and single-stage techniques are unsuitable with porous, chemically inert materials. Specimens were prepared by crushing the alumina pellets with an agate mortar and pestle and suspending the powder in butyl alcohol. Drops of the suspension were placed onto the electron microscope grids previously coated with a carbon support film. These specimens were ready for examination after evaporation of the butyl alcohol in a vacuum of 5×10^{-5} torr.

Examination was carried out with a J.E.M. 6A electron microscope manufactured by Japan Electron Optics Laboratory Co., Ltd. This microscope is a high-resolution instrument with a resolving power better than 10 Å and was operated



FIG. 2. Electron micrograph of activated alumina, showing irregularly shaped macropores. 35 000 \times .

at an accelerating voltage of 100 kV. Small areas of the catalyst particles were transparent at 100 kV and the pores were in reasonable contrast at an electron optical magnification of 80 000 \times .

RESULTS

At low magnifications (35 000 \times) the catalyst appeared as discrete particles

separated by large fissures (Fig. 2). Smaller holes of irregular shape were observed in some particles although no regularity in their size was apparent. Most of each particle was dense to the electron beam with the exception of the thinner edges. At higher magnifications (800 000 \times) these transparent edges were seen to contain a regular pattern of small pores (Fig. 3).

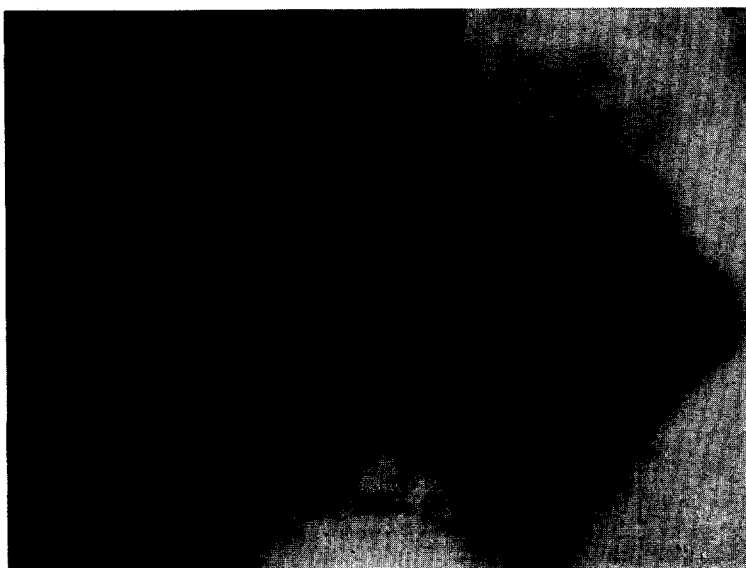


FIG. 3. Electron micrograph of activated alumina, showing micropore structure. 800 000 \times .

The best contrast was obtained with particles so oriented that rows of pores were observed at 60° to each other. These areas were used for measuring pore dimensions but, even so, there was no sharp line of contrast at the pore–solid interface and exact measurements were not possible.

It seems that three types of pores can be distinguished in the micrographs:

1. large spaces *between* discrete particles, having no apparent characteristic size or shape;
2. smaller irregular holes *in* the particles;
3. a regular array of uniform micropores arranged hexagonally.

The following method was used to obtain mean micropore diameters from four separate particles. Two diameters at right angles were determined for each pore by measurement with a vernier rule (each division, 0.1 mm) on a photographic print at a total magnification of $800\,000\times$. The print was illuminated from the back in order to facilitate the estimation of the pore/solid boundary. Since there were no significant differences between the diameters at right angles an average diameter for each pore was obtained. The mean of at least 25 pores measured over various areas on each particle was determined. Limits for each mean were derived by conventional statistical analysis for 99.9% confidence limits (14). Errors in the magnification of the electron microscope ($\pm 2\%$) are less than the limits set. In order to test the reliability of measurement additional measurements of the pores on Particle 1 were made several days later and by two different persons. No significant difference was observed between the additional measurements and those made initially. The results are shown in Table 1. A mean micropore diameter of 27 \AA is used in the calculations.

Micropore densities for the four particles were determined from the same photographic print. Initially, the number of pores in a small square area of the print was counted. This method yielded a very small count since the lack of contrast and lack

of uniform transparency away from the edges of the particle necessitated a small counting area. The final results were obtained from the product of the number of pores cut by two perpendicular cross lines each 5 cm long, so positioned that areas

TABLE 1
MEASUREMENTS OF PORE DIAMETERS AND
DENSITIES TAKEN FROM THE MICROGRAPHS

Particle	Mean micropore diameter (\AA)	Mean micropore densities per cm^2
1	28 ± 2	32.1×10^{11}
2	27 ± 1	35.6×10^{11}
3	27 ± 1	37.0×10^{11}
4	26 ± 2	37.4×10^{11}

in good contrast were included. The micropore densities, determined from five different areas in each particle (Table 1), enable estimates of the pore spacing λ to be made from the equation

$$\lambda^2 = 2/3^{1/2}n$$

where n is the number of micropores per unit area of external surface.

DISCUSSION

Interpretation of Micrographs

Because of the irregular nature of the large spaces between particles and of the medium size spaces within particles, it was not possible to obtain an explicit measure of the contributions to total surface area and voidage by those spaces. The micrographs had shown that an estimate of voidage and surface area on the basis of the micrographs alone was not going to be achieved. It would be possible, nevertheless, to adopt a realistic model of pore structure for use in the conventional calculations.

The regular micropores seemed capable of interpretation in one of three ways:

1. The pores are parallel, with lengths greater than their diameter, polygonal in cross section. It is unlikely that their section is circular if they are formed by the rupture of the molecular structure.

2. The pores are the interstices between parallel rods of solid.

3. The pores are the interstices between packed spheres of solid.

The third of these possibilities implies a symmetry in a third direction and was effectively discounted after experiments in which the specimen was tilted relative to the electron beam. With increasing angle of tilt, the contrast at the pore-solid boundary will reduce in a direction perpendicular to the tilt axis, forming, eventually, large pore chains for pore models 1 and 2 whereas no consistent effect will be observed for model 3. Using the stereo stage in the electron microscope, tilting within the range 0° to 6° was found to change the contrast in one direction producing, long pore chains as predicted for models 1 and 2. The second model was rejected after a closer examination of the micrographs had shown that it was not possible to obtain a dimension characteristic of the solid, certainly nothing consistent with the idea of a solid rod. By contrast, and in spite of the lack of definition at the gas-solid interface, it was possible to obtain measurements of pore diameters with a surprisingly consistent accuracy. Consequently, the first model was taken as correct, and because of the regular pattern of pores, the calculation of pore volume and surface area contributed by the micropores was relatively straightforward.

In the micropore region,

$$\text{Surface area per g} = n\pi a / \rho_s (1 - \epsilon_1)$$

$$\text{Voidage} = n\pi a^2 / 4\rho_s (1 - \epsilon_1)$$

where ρ_s is the real density of alumina and ϵ_1 is the voidage in the micropore region.

The irregular pores of both kinds will be termed collectively "macropores." Though they cannot be described by any simple model, it will be assumed that they are characterized by the diameter a of an equivalent cylinder having a numerical density ν per unit area (analogous to n) and a voidage ϵ_2 .

If the alumina is thought of as consisting

of two regions, one containing a uniform distribution of the observed micropores and the other containing the macropores plus any nonporous alumina that may exist, and if, in addition, the ratio of the first region to the second is taken as $1:\delta$, the following analysis becomes possible. The surface area per g (S) of total alumina is

$$S = \frac{n\pi a + \delta\nu\pi a}{(1 - \epsilon_1)\rho_s + \delta(1 - \epsilon_2)\rho_s} = \frac{n\pi a}{\rho_s} \left[\frac{1 + (\delta\nu a / \eta a)}{(1 - \epsilon_1) + \delta(1 - \epsilon_2)} \right] \quad (1)$$

Also for voidage

$$(\epsilon_1 + \delta\epsilon_2) / (1 + \delta) = \epsilon$$

Substitute for $(1 - \epsilon_1)$ in Eq. (1)

$$S = \frac{n\pi a}{\rho_s(1 - \epsilon)} \left[\frac{1 + \delta\nu a / na}{1 + \delta} \right] \quad (2)$$

where the term outside the bracket gives the surface area if the whole of the voidage were contributed by micropores, i.e., $\delta = 0$. Since $\epsilon = (\rho_s - \rho_a) / \rho_s$, where ρ_a is the apparent density of the alumina, Eq. (2) may be rewritten

$$S = \frac{n\pi a}{\rho} \left[\frac{1 + (\delta\nu a / na)}{1 + \delta} \right] \quad (3)$$

The term in brackets is the correction to be applied for the presence of macropores. The correction will be small if δ be small or if $\nu a \approx na$.

The following data were obtained for the commercial alumina (15):

$$\rho_a = 1.15 \text{ g/cc}$$

$$\rho_s = 2.75 \text{ g/cc}$$

$$S_{\text{BET}} = 275 \text{ m}^2/\text{g}$$

From Table 1

$$n = 35.5 \times 10^{11}$$

$$a = 27 \text{ \AA}$$

The term outside the bracket in Eq. (3) becomes $262 \text{ m}^2/\text{g}$. It follows that the correction term in the bracket is approximately unity. Since the micrographs show that δ is finite, $\nu a / na \approx 1$.

The equality of na and νa means that micro- and macropores contribute to the

available surface area in the ratio 1:8 since Eq. (3) may be rewritten

$$S = \frac{n\pi a}{\rho_a(1 + \delta)} + \frac{\delta\nu\pi\alpha}{\rho_a(1 + \delta)}$$

The relative contributions to voidage follow from

$$(\epsilon_1 + \delta\epsilon_2)/(1 + \delta)$$

and

$$\epsilon_1 = \frac{1}{4}n\pi a^2, \quad \epsilon_2 = \frac{1}{4}\nu\pi\alpha^2$$

Micro- and macropore contributions are in the ratio $a:\delta\alpha$.

Surface Area by the t Method

In their work on pore systems in catalysts (4), de Boer and co-workers used an expression relating the statistical thickness t of an adsorbed layer to the volume V_a of gas adsorbed at STP.

For a flat surface

$$t = X/S$$

where X is the liquid volume of adsorbate. For nitrogen at its boiling point,

$$V_a = (S/15.47) t \quad (4)$$

t values were obtained for aluminas from tabulated values of t and relative pressures p/p_0 on samples of known surface areas. Values of V_a , the gas volume adsorbed at STP, were obtained from adsorption isotherms. A plot of V_a against t would be expected to give a straight line through the origin as long as the surface area remained constant and the adsorbate built up in equal layers.

Applying the method to the isotherm of Fig. 1 and using the t values tabulated in ref. (4), Fig. 4 was drawn.

The interpretation of the t plot of the commercial alumina, especially with respect to the areas associated with the smallest pores, must be viewed with caution. The linearity of the plot before the onset of capillary condensation depends on the constancy of the surface area available for adsorption. As adsorption proceeds in pores of 27-Å diameter, the effective surface area of those pores decreases rapidly. The fact that the slope of Fig. 4

does not decrease initially may indicate that the effect is largely offset by conditions in the macropores. Subsequently, capillary condensation in the micropores

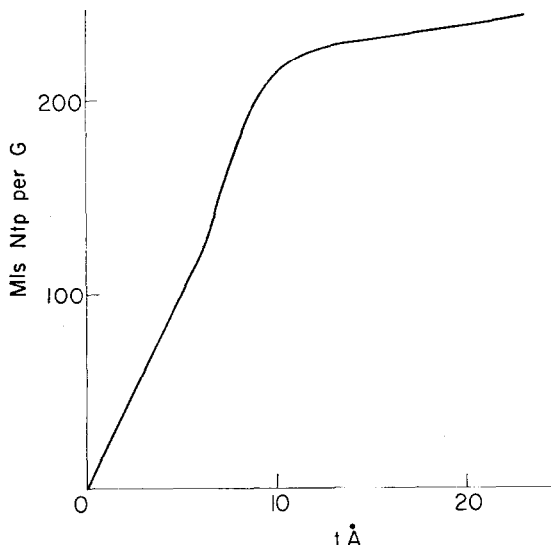


FIG. 4. t diagram plotted from data in ref. (4) and the adsorption isotherm. Abscissa, thickness of the adsorbed layer; ordinate, volume of nitrogen referred to NTP, adsorbed on 1 gram of solid.

and in the smaller macropores reverses the tendency for the slope to decrease until such times as the decrease in area of the macropore system becomes the predominant factor.

The increase in slope of the line through the origin, at a value of $t = 6$ Å, is consistent with the onset of capillary condensation occurring in sufficient proportions to offset the decrease in available surface occurring through adsorption. The relative pressure p/p_0 corresponding to this t is 0.44 and since it is the adsorption branch being considered, the Cohan radius (r_c) will be calculated (16)

$$r_c = \frac{-2\sigma V}{2RT \ln(p/p_0)}$$

where, for nitrogen,

$$\begin{aligned} \sigma &= 8.72 \text{ dynes/cm} \\ V &= 34.68 \text{ cm}^3/\text{mole} \\ T &= 78^\circ\text{K} \end{aligned}$$

and, therefore,

$$r_c = 5.7 \text{ \AA}$$

Assuming the condensation to occur first in pores approximately cylindrical, the diameter of the pores is given by $2(r_c + t)$ which is 23.4 \AA . The surface blocked off as a result of condensation causes the slope of the curve to be reduced. The slope decreases until t has reached a value of about 13.8 \AA , corresponding to a relative pressure of 0.88, and a total pore diameter of $2(13.8 + 36.2) = 100 \text{ \AA}$.

The second linear portion of the curve suggests the existence of large macropores in which no condensation occurs.

From the slope of the first linear portion, a surface area of $291 \text{ m}^2/\text{g}$ is predicted which agrees well enough with the BET estimate. From the slope of the second linear portion, a surface area of $18 \text{ m}^2/\text{g}$ associated with the large macropores is calculated.

If the large macropores are those thought, from the micrographs, to lie *between* particles then a mean radius R of these particles can be found if they are assumed to be spherical.

Let the number of particles per gram be N . Then

$$N4\pi R^2 = 18 \times 10^4 \text{ cm}^2$$

and

$$N\frac{4}{3}\pi R^3\rho = 1$$

so

$$R = 1/(6 \times 10^4\rho)$$

The density of the particle ρ is not known since the particles enclose some small macropores. But the density must lie between 1.15 and 2.75 g/cc ; therefore $1450 \text{ \AA} > R > 605 \text{ \AA}$.

The failure of the nitrogen isotherm of Fig. 1 to indicate an abundance of pores of 27 \AA diameter is noteworthy. On the basis of the Kelvin equation, and assuming one distribution of cylindrical pores, the steep portion of the desorption branch, occurring at $p/p_0 \approx 0.5$ corresponds to a pore diameter of about 40 \AA . Again, the slope of the adsorption branch of the iso-

therm shows no preference for 27 \AA . It has been suggested elsewhere (17) that a shallow slope of an adsorption branch does not necessarily indicate a distribution of pore sizes. It may be the result of some other effect such as heat of adsorption.

The interpretation of the isotherm on the basis of the Kelvin or the Cohan equation, appears to obscure the separate effects of the three types of pores.

CONCLUSIONS

From the study of micrographs of a sample of commercial activated alumina, a picture emerges of a structure which incorporates some regions of well-ordered pores and others of random pores.

The well-ordered pores are approximately cylindrical in cross section and a number of measurements give a mean diameter of $27 \pm 1 \text{ \AA}$. These pores are arranged hexagonally at a repeat distance λ calculated to be 58 \AA .

The random pores are bigger but have no characteristic shape or size. It appears, however, that they may be of two types, those within individual particles of alumina that agglomerate to make a granule, and those between such particles.

When the random or macropores are arbitrarily characterized by an equivalent cylinder of diameter α and number density ν , an expression for surface area can be obtained which can be compared with the BET surface. The comparison suggests that the micro- and macropores contribute to the total surface area in the ratio $1:\delta$, where δ is the extent of the macropore region associated with unit extent of the micropore region. Though it was not possible to measure δ on the micrographs, it is clear that both micro and macropores contribute significantly to the surface area. The voidage, on the other hand, would appear to stem chiefly from the macropores, which contribute in the ratio $\delta\alpha$ to a compared with the micropores.

A t plot suggests the existence of large macropores in which no condensation occurs and with which an area of $18 \text{ m}^2/\text{g}$ is associated. If it be the large macropores which lie between the agglomerated

particles constituting the granule, a mean size of particle can be calculated. Assuming the particles are spherical, a diameter of the order of 2000 Å is obtained.

REFERENCES

1. DE BOER, J. H. The shape of capillaries. In "The Structure and Properties of Porous Materials" (D. H. Everett and F. S. Stone, eds.). Butterworth, London, 1958.
2. INNES, W. B., *Anal. Chem.* **29**, 1069 (1957).
3. CRANSTON, R. W., AND INKLEY, F. A., *Advan. Catalysis* **9**, 143 (1957).
4. LIPPENS, B. C., LINSON, B. G., AND DE BOER, J. H., *J. Catalysis* **3**, 32 (1964).
5. DERJAGUIN, B. V., "Solid/Gas Interface." *Proc. Intern. Congr. Surface Activity, 2nd, London, 1957*, p. 153 Butterworths, London, 1957.
6. DE BOER, J. H., "Solid/Gas Interface." *Proc. Intern. Congr. Surface Activity, 2nd, London, 1957*, p. 93. Butterworths, London, 1957.
7. SOUZA SANTOS, P., VALLEJO-FREIRE, A., AND SOUZA SANTOS, H. L., *Kolloid-Z.* **133**, 101 (1953).
8. MOSCOU, L., AND VAN DER VLIES, G., *Kolloid-Z.* **163**, 35 (1959).
9. DAY, M. K. B., AND HILL, V. J., *J. Phys. Chem.* **57**, 946 (1953).
10. PAPÉE, D., AND TATIAN, R., *Bull. Soc. Chem.*, p. 983 (1955).
11. BOOKER, C. J. L., WOOD, J. L., AND WALSH, A., *Brit. J. Appl. Phys.* **8**, 347 (1957).
12. BOWEN, J. H., AND DONALD, M. B., *Chem. Eng. Sci.* **18**, 599 (1963).
13. BRADLEY, D. E., "Techniques for Electron Microscopy" (D. Kay, ed.). Blackwell Sci. Publ., Oxford, 1961.
14. BROWNLEE, K. A. "Industrial Experimentation," p. 32. H. M. Stationery Office, London, 1957.
15. "Activated Alumina," Catalogue of Peter Spence & Sons Ltd. Widnes, Lancs., England.
16. COHAN, L. H., *J. Am. Chem. Soc.* **60**, 433 (1938).
17. IMELIK, B., "The Structure and Properties of Porous Material" (D. H. Everett and F. S. Stone, eds.), p. 135. Butterworth, London, 1958.